Liquid Crystals
Publication details, including instructions for authors and subscription information:
http://www.informaworld.com/smpp/title~content=t713926090

Synthesis, mesomorphic properties and crystal structure studies of a chiral ferroelectric liquid crystal series

H. Allouchi; M. Cotrait; M. Laguerre; J. C. Rouillon; J. P. Marcerou; H. T. Nguyen

Online publication date: 06 August 2010

To cite this Article Allouchi, H. , Cotrait, M. , Laguerre, M. , Rouillon, J. C. , Marcerou, J. P. and Nguyen, H. T.(1998) 'Synthesis, mesomorphic properties and crystal structure studies of a chiral ferroelectric liquid crystal series', Liquid Crystals, 25: 2, 207 — 215
To link to this Article: DOI: 10.1080/026782998206353
URL: http://dx.doi.org/10.1080/026782998206353

LIQUID CRYSTALS, 1998, VOL. 25, NO. 2, 207–215

Synthesis, mesomorphic properties and crystal structure studies of a chiral ferroelectric liquid crystal series

by H. ALLOUCHI
Laboratoire de Chimie Physique, Faculté de Pharmacie, 31 Av. Monge, 37200 Tours, France

M. COTRAIT
Laboratoire de Cristallographie, Université de Bordeaux I, 351 Cours de Libération, 33405 Talence Cedex, France

M. LAGUERRE, J. C. ROUILLON, J. P. MARCEROU and H. T. NGUYEN*
Centre de Recherche Paul Pascal (CNRS), Université de Bordeaux I, Avenue A. Schweitzer, 33600 Pessac, France

(*Received 6 February 1998; accepted 9 March 1998*)

A new series of chiral mesogens: (*R*) 4-(1-methylheptyloxycarbonyl)phenyl 4-(4-alkyloxyphenyl)-ethylylbenzoates—has been synthesized. All materials are mesomorphic and the liquid crystalline properties were characterized by optical observation, DSC and electro-optical measurements. They display SmA and ferroelectric SmC* phases at low temperatures. One of them, the nonyloxy derivative, exhibits the SmC^*_α phase, present in different 'antiferroelectric' series. This behaviour is confirmed by mixture studies. Furthermore one compound of the series, the heptyloxy derivative, $C_{37}H_{48}O_5$ crystallizes in the P_{21} space group ($Z=2$) with the following parameters: $a=8{\cdot}497$ (1), $b=5{\cdot}490$ (1), $c=36{\cdot}148$ (4) Å with $\beta=92{\cdot}72$ (1)°. The final R and wR reliability factors were equal to 0·109 and 0·124, respectively; the goodness of fit was equal to 3·0. The whole molecule is L-shaped with the long chiral chain almost perpendicular to the core moiety as observed for several compounds showing an antiferroelectric mesophase. In the crystal, the molecules related through the 2_1 axis, located at $z=0{\cdot}5$, give an antiparallel smectic C-like arrangement. The thickness of the sheets is equal to the c parameter, with a tilt angle close to 35°. There are strong intersheet interactions between the chiral chains related through the 2_1 axes located at $z=0$ and 1.

1. Introduction

During the last twenty years, after the first observation of the ferroelectric smectic C* (SmC*) phase by Meyer *et al.* [1] in 1975 and its surface stabilized electro-optical properties by Clark and Lagerwall [2] in 1980, the search to find new materials has increased. Additionally, the discovery of the antiferroelectric smectic C* (SmC^*_A) phase by Chandani *et al.* [3] in 1989 and its sub-phases has also stimulated the search for new materials [4–10] in this field, not only for device applications but also for fundamental studies. The latter materials have the general formula:

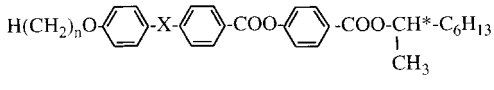

I

where X = –(single bond), –C≡C–, COO–, COS–.

*Author for correspondence.

It is clear that with X more or less rigid, the antiferroelectric SmC^*_A phase is always observed. The flexible 1,2-diarylethane core, well known to induce tilted smectic phases [11, 12] and quite suitable to obtain wide SmC* temperature ranges, is however used in this report to study the influence of the flexible CH_2–CH_2 linking group on the existence of the antiferroelectric SmC^*_A phase.

In this paper we describe the synthesis, characterization, electro-optical properties and crystal structure of members of a homologous series having the general formula:

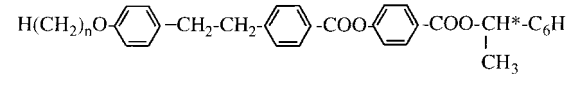

II

2. Synthesis

The chiral diarylethane series was prepared following the scheme shown below.

0267–8292/98 $12·00

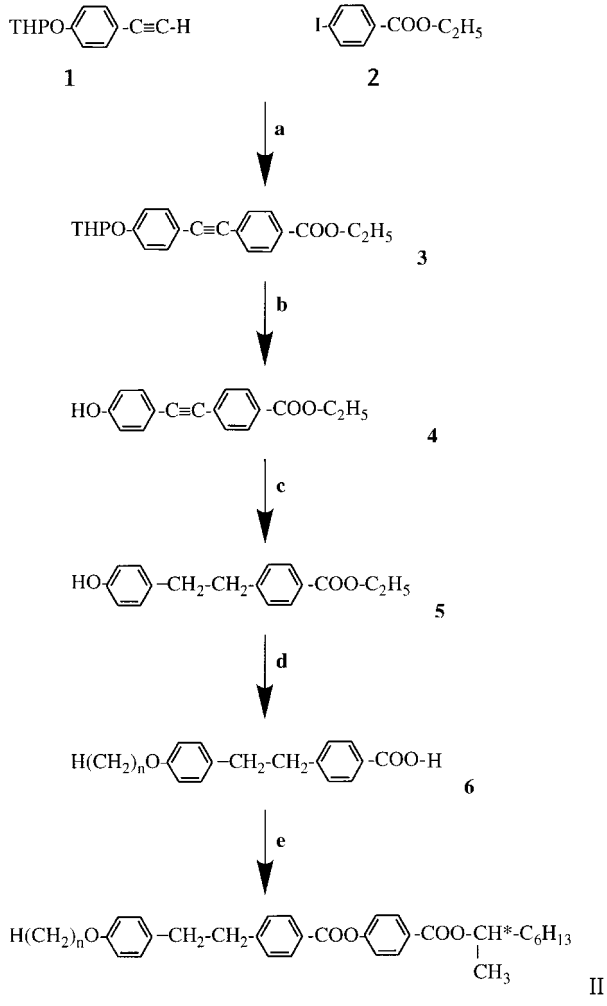

Scheme.

(a) $PdCl_2$, $Cu(AcO)_2$, H_2O, Ph_3P, iPr_2NH
(b) PTSA, MeOH, CH_2Cl_2
(c) H_2, Pd/C, C_2H_5OH 95%
(d) $C_nH_{2n+1}Br$, KOH, EtOH; KOH; HCl, H_2O
(e) (R) 4-HO-Ph-COO-CH*(CH_3)C_6H_{13}, DCC, DMAP, CH_2Cl_2

3. Mesomorphic characterization

All the final compounds were purified on silica gel with toluene as eluent and were recrystallized from absolute ethanol. They are mesomorphic and display SmA and/or SmC* and SmI_A^* phases. One of them, the nonyloxy derivative exhibits between the SmA and SmC* phases a SmC_α^* phase. Their thermal behaviour was investigated by differential scanning calorimetry (Perkin Elmer DSC7) and the phase identification was carried out by thermal optical microscopy using a Zeiss Ortholux polarizing microscope equipped with a Mettler FP5 hot stage. The liquid crystal transition temperatures and enthalpies for the series are given in table 1.

In most cases, on cooling from the isotropic liquid, one can observe fan-shaped or homeotropic textures of the SmA phase and on further cooling the SmC* phase with broken and striated fan-shaped textures. The SmI_A^* phase was obtained with mosaic or striated fan-shaped textures. It is very difficult to detect the SmC_α^* phase by optical observation because its textures are similar to those of SmA. Its presence was confirmed by DSC, electro-optical measurements and miscibility studies. None of the materials display the SmC_A^* or SmC_{FI}^* phases; we will discuss this behaviour in the next section.

4. Polarization, response time and soft mode contribution

The spontaneous polarization and the response time were measured in the smectic I_A^* and smectic C* phases by applying a square wave of $\pm 10{\cdot}5$ V, at a frequency of 300 Hz, on a sample aligned in the bookself geometry in a 6 μm thick commercial cell (from E.H.C. Japan). In the smectic C* phase (see figure 1), the polarization follows a classical $(T_c - T)^{0{\cdot}5}$ law with a saturation at about 80 nC cm^{-2}, while in the smectic I_A^* phase, the apparent polarization is slightly lower, due to the increased rigidity. This is also illustrated by the response time, measured by the half width of the polarization peak (figure 1), which varies smoothly in the C* phase while it diverges in the smectic I_A^* phase up to 0·9 s at 33°C.

The angle from the normal to the layers in the smectic phases is measured in the classical way at very low frequency (0·1 Hz). This tilt angle increases quickly from the SmC_α^*–SmC* transition and reaches a value of about 25° (figure 2).

In the smectic C* and smectic A phases, conversely, a triangular wave was used in order to reveal the characteristic two peak shape in the smectic C_α^* phase. This allowed us to determine the soft mode contribution

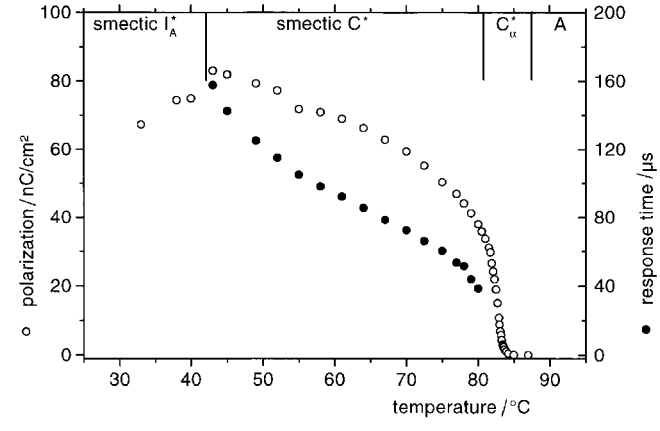

Figure 1. Plot of the spontaneous polarization in the smectic I_A^*, C* and C_α^* phases (open circles) as a function of temperature, and the response time (solid circles) for an applied field of 17·5 V cm^{-1}.

Table 1. Transition temperatures (°C) and enthalpies in italics (kJ/mol) of members of series II.

	Phase										
n	Cr		SmI_A^*		SmC*		SmC_α^*		SmA		I
7	•	66·5	•	(47)	•	69·4	—		•	90	•
		41		*1·3*		*0·02*				*8·2*	
8	•	54	•	(47)	•	77	—		•	91·2	•
		25		*1·5*		*0·1*				*9·1*	
9	•	55	•	(42)	•	82·3	•	84	•	89	•
		27		*1·2*		*0·17*[a]				*8·9*	
10	•	49	•	(39)	•	84·8	—		•	88·6	•
		23·7		*1·2*		*0·18*				*9·2*	
11	•	46	•	(35)	•	86	—		—		•
		41		*1·3*		*10*					
12	•	52	•	(32)	•	86	—		—		•
		40		*1·15*		*9·4*					

[a] The sum of SmA–SmC_α^* and SmC_α^*–SmC* transition enthalpies.

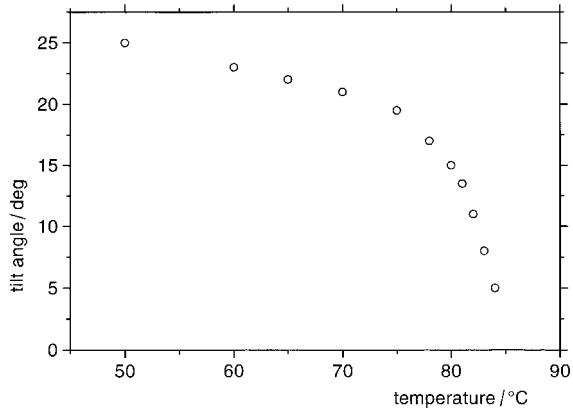

Figure 2. Tilt angle θ versus $T_{SmC*-SmA} - T$ for II ($n = 9$).

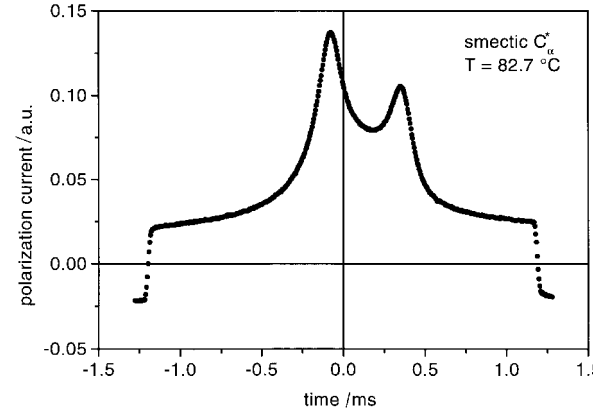

Figure 3. Current versus time in a half period of the applied triangular field ($\pm 13{\cdot}0$ V cm^{-1}). The two peaks are characteristic of the smectic C_α^* phase, while the height of the baseline gives access to the soft mode contribution to the dielectric constant.

to the dielectric constant in the vicinity of the smectic C_α^* to smectic A transition. The typical response is illustrated in figure 3.

In this figure, one sees the time evolution of the current in the cell when the applied voltage goes from -8 V (at time $\sim -1{\cdot}2$ ms) to $+8$ V (at time $\sim +1{\cdot}2$ ms). The polarization starts with the saturated value $-P_s$ in the induced smectic C* phase, then after the first current peak it goes to a positive intermediate value $+P_i$ and finally to the saturated $+P_s$. When the second peak appears, close to the smectic C* phase, it is much smaller than the first one, indicating that $+P_i$ is smaller than but close to $+P_s$ (this is reminiscent of ferrielectric behaviour). On further heating, the second peak increases and becomes equal to the first (antiferroelectric behaviour). Eventually, the height of the plateau below the peaks gives information on the soft mode contribution as plotted in figure 4.

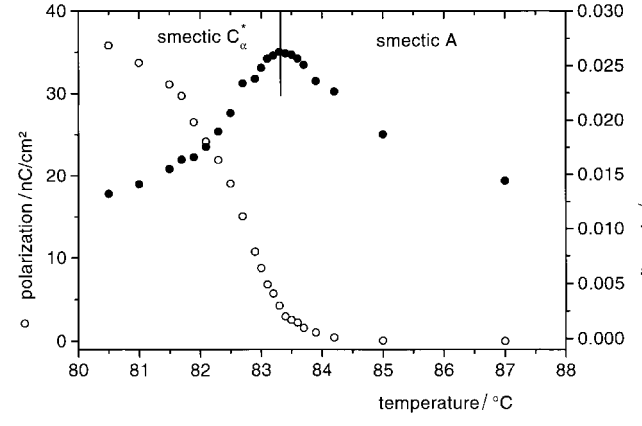

Figure 4. Saturated polarization P_s in the induced ferroelectric phase (open circles) and baseline of the current curve (solid circles), proportional to the dielectric constant.

5. Crystal structure

During the last decade several crystal structures of mesogenic compounds with chiral alkyl chains have been published [13–23]. Most of them show a SmC* ferroelectric mesophase. Three types of compound with a core containing biphenyl ester moieties were chosen for study since their mesophase characteristics had already been examined [13]. About half of them had a short chiral 2-methylbutyl group [13–16, 19, 22]. None of the latter compounds gives rise to the antiferroelectric SmC_A^* mesophase. We recently published the crystal structures of two compounds with a completely different core and with short and polar chiral chains, namely 2-chloro-3-methylpentanoyloxy and 2-chloro-3-methylbutanoyloxy [24, 25].

The remaining structures published by Hori *et al.* have either a 1-methylheptyloxy chiral chain [17, 18, 20, 23] or a 1-methyl(pentyloxy or hexyloxy) chiral chain [21]. Four of the latter compounds present a SmC_A^* antiferroelectric mesophase [20, 21, 23]. This is also the case for the 4-(1-methylheptyloxycarbonyl)phenyl 4-heptyloxytolane-4-carboxylate on which we recently published [26, 27]. In this paper we study the crystal structure of the nonyloxy derivative.

Colourless prismatic crystals were grown by slow evaporation of chloroform solutions. The compound studied, $C_{37}H_{48}O_5$, $Mx = 572{\cdot}8\ g\ mol^{-1}$, crystallizes in the monoclinic system, space group $P2_1$ ($Z = 2$). The unit-cell parameters were obtained by a least squares fit of the setting angles of 25 reflections with θ between 25° and 42° and are as follows: $a = 8{\cdot}497\ (1)$, $b = 5{\cdot}490\ (1)$, $c = 36{\cdot}148\ (4)$ Å and $\beta = 92{\cdot}72\ (1)°$ with a cell volume of 1684 $Å^3$. The calculated density is $1{\cdot}129\ g\ cm^{-3}$ and is rather low as is the case for most mesogenic compounds. The linear absorption coefficient is $\mu = 0{\cdot}588\ mm^{-1}$.

The diffracted intensities were collected with a CAD-4 Enraf-Nonius diffractometer equipped with a graphite monochromator for $\theta_{max} = 60°$: $9 \geqslant h \geqslant -9$, $6 \geqslant k \geqslant 0$, $40 \geqslant l \geqslant 0$. Three standard reflections were used to monitor the data collection and detect any decrease of intensity ($-3\ 2\ 8$, $-4\ 2\ 9$, $-3\ 2\ 5$): the transmission factor $T(h\ k\ l)$ lies between 0·95 and 1·0, nevertheless the crystal absorption correction was made using the ψ scan technique [28]. There were 2807 independent reflections of which 1248 were considered as observed [$I > 2\ sig(I)$ and $R_{int} = 0{\cdot}016$].

The crystal structure was solved with some difficulty using the SHELXS86 program [29]; several successive Fourier syntheses were necessary to generate the whole molecule which was refined thanks to the SHELXL93 package [30] using constraints on a few bond lengths.

Scattering factors were taken from the *International Tables of Crystallography* [31]. The hydrogen atoms were introduced in their theoretical positions and allowed to ride with the atoms to which they are attached; the refinement was then resumed. The final reliability factors were $R = 0{\cdot}109$ and $wR = 0{\cdot}124$. These rather high values can be related to some disorder and quite high atomic motion factors.

6. Theoretical calculations

The partial punctual electronic charges were calculated with the MOPAC 6.0 package, using the MNDO method. The calculations were performed on a SGI Indy R4400 Silicon Graphics station, using molecular mechanics with the CVFF (Consistent Force Field) method [32].

The starting conformations were those found in the crystal structure for the present material and the structure of a chiral compound [(*S*)-(1-methylheptyl) 4-(4-octyloxy-3-fluorobenzoyloxy)tolane-4′-carboxylate)], named C8F Tolane, which does not present any SmC* or SmC_A^* mesophase [33]. As we had already observed, preliminary attempts showed that gradient conjugate minimization methods led to a large distortion of the crystalline conformation for an isolated molecule. In the present case, where it is essential to preserve the crystalline conformation, the best minimization method is the steepest descent (SD). This procedure was performed without any distance cut off† (the electrostatic interactions are significant even at a large distance) until the energy variation was less than 0·02 kcal cycle (3000 cycles): the root mean square was less than 0·3 Å at the end of the calculation.

The intersheet energy was evaluated by taking into account three sheets with a limited number‡ of molecules per sheet, and by calculating the binding energy between the middle sheet on one side and between the lower and upper sheets on the other side.

7. Discussion

All the compounds of series II show low clarification temperatures. They do not display SmC_A^* or SmC_{FI}^* phases, but the tendency to give them is marked as shown by the mixture study. At first the SmC_α^* phase is observed in a pure compound, the nonyloxy derivative, and the others are put in evidence for different mixtures between this nonyloxy material and the well known C8 tolane as MHPOBC and exhibiting polymesomorphism with two SmC_{FI}^* phases between SmC_A^* and SmC*

† The cut-off distance is the interatomic distance above which the calculations are no longer performed.

‡ The rigorous evaluation of the intersheet energy should involve a much greater number of molecules in every sheet to limit the effects of series endings. Our calculations already involve a great number of molecules, a very large number of interacting pairs and a long calculation time because of the minimization of the optimal conformation of all molecules.

phases. The 50–50 mixture by weight between these two compounds gives the sequence:

$$SmI_A^* \ 56 \ SmC_A^* \ 82 \ SmC_{FI}^* \ 87{\cdot}3 \ SmC^* \ 96{\cdot}2$$

$$SmC_\alpha^* \ 97{\cdot}1 \ SmA \ 114 \ I \ (°C)$$

This not only shows all the phases of the C8 tolane but also the miscibility between the SmC_α^* phase and the SmI_A^* phase of these two compounds. We would also like to note that DSC does not clearly show two ferrielectric phases in the mixture because the transition enthalpy is very weak. All these phases are still observed in the 75% II ($n=9$)–25% C8 tolane mixture. This behaviour confirms the tendency of series II materials to give the smectic C_A^* 'antiferroelectric' phase as evidenced by the crystal structure study.

The fractional x, y, z coordinates and the equivalent U_{eq} thermal motion factors are listed in table 2. The U_{eq} values for the carbons of the chiral chain are quite high, which is not the case for those of the heptyloxy terminal chain. The molecular conformation along with the atom labelling is presented in figure 5. The bond lengths are given in table 3 and agree quite well with the literature.

The lengths of the core (atoms O26 to C27), of the heptyloxy chain (atoms O26 to C33) and the CH_3–C*HC_6H_{13} chiral chain (atoms C43 to C44) are respectively equal to 20·46 (3), 8·73 (3) and 8·52 (3)Å. The chiral chain makes an angle close to 100° with

Table 2. Atomic coordinates and equivalent U_{eq} thermal motion factors.

Atom	x/a	y/b	z/c	U_{eq}
C1	0·2424 (23)	0·2500 (45)	0·7849 (5)	0·063 (14)
C2	0·1538 (25)	0·0541 (46)	0·7733 (5)	0·068 (14)
C3	0·0889 (21)	0·0469 (41)	0·7369 (5)	0·056 (13)
C4	0·1194 (22)	0·2401 (39)	0·7143 (5)	0·053 (12)
C5	0·2132 (25)	0·4314 (46)	0·7250 (5)	0·068 (15)
C6	0·2789 (24)	0·4337 (48)	0·7606 (5)	0·072 (15)
O7	0·0555 (16)	0·2223 (29)	0·6774 (3)	0·066 (9)
C8	−0·0472 (22)	0·4003 (43)	0·6661 (5)	0·057 (13)
O9	−0·0822 (17)	0·5702 (33)	0·6836 (3)	0·080 (10)
C10	−0·1096 (22)	0·3483 (39)	0·6268 (5)	0·051 (12)
C11	−0·2233 (23)	0·5078 (40)	0·6116 (5)	0·061 (13)
C12	−0·2826 (23)	0·4619 (45)	0·5758 (5)	0·062 (13)
C13	−0·2360 (22)	0·2665 (42)	0·5558 (5)	0·058 (13)
C14	−0·1274 (23)	0·1117 (40)	0·5716 (5)	0·059 (13)
C15	−0·0661 (24)	0·1441 (46)	0·6075 (5)	0·070 (15)
C16	−0·3005 (24)	0·2329 (47)	0·5164 (5)	0·065 (14)
C17	−0·1871 (22)	0·3319 (46)	0·4883 (5)	0·064 (14)
C20	−0·2521 (22)	0·3189 (44)	0·4487 (5)	0·060 (14)
C21	−0·3502 (25)	0·5017 (47)	0·4349 (5)	0·070 (15)
C22	−0·4167 (23)	0·4993 (41)	0·3992 (5)	0·058 (13)
C23	−0·3771 (22)	0·3136 (40)	0·3765 (5)	0·053 (12)
C24	−0·2790 (22)	0·1308 (41)	0·3889 (5)	0·058 (13)
C25	−0·2185 (25)	0·1357 (45)	0·4252 (5)	0·070 (15)
O26	−0·4332 (17)	0·2921 (29)	0·3397 (3)	0·072 (10)
C27	−0·5238 (24)	0·4965 (46)	0·3256 (5)	0·070 (15)
C28	−0·5615 (22)	0·4525 (41)	0·2841 (5)	0·055 (12)
C29	−0·6517 (23)	0·6703 (44)	0·2683 (5)	0·064 (14)
C30	−0·6954 (24)	0·6568 (48)	0·2270 (5)	0·071 (15)
C31	−0·7726 (24)	0·8875 (50)	0·2127 (5)	0·073 (15)
C32	−0·8244 (26)	0·8663 (51)	0·1717 (6)	0·083 (17)
C33	−0·9024 (33)	1·1025 (59)	0·1582 (6)	0·106 (20)
C34	0·3166 (25)	0·2601 (46)	0·8245 (5)	0·070 (15)
O35	0·2781 (19)	0·0727 (37)	0·8445 (3)	0·097 (12)
O36	0·4003 (22)	0·4244 (39)	0·8342 (4)	0·116 (14)
C37	0·3534 (35)	0·0704 (62)	0·8826 (6)	0·114 (21)
C38	0·2424 (38)	−0·0361 (106)	0·9064 (7)	0·188 (37)
C39	0·1010 (41)	0·1026 (131)	0·9129 (8)	0·237 (48)
C40	0·0086 (78)	0·1027 (140)	0·9406 (9)	0·323 (69)
C41	−0·1307 (59)	0·2756 (109)	0·9453 (9)	0·223 (44)
C42	−0·2420 (96)	0·1724 (100)	0·9723 (12)	0·354 (71)
C43	−0·3578 (68)	0·3837 (128)	0·9711 (11)	0·280 (58)
C44	0·4983 (38)	−0·0935 (81)	0·8800 (48)	0·151 (29)

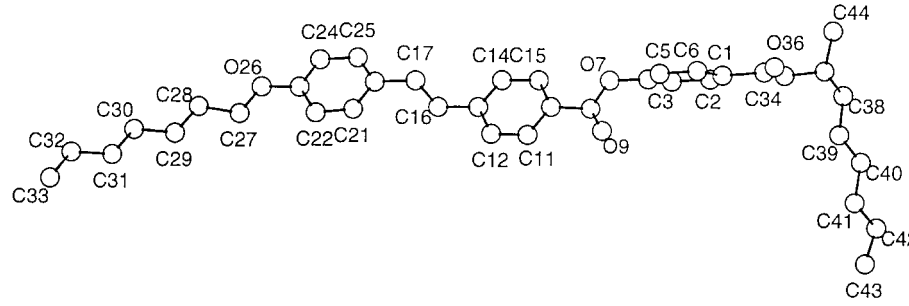

Figure 5. Conformation of the molecule and atom labelling.

Table 3. Bond lengths (Å) with standard deviations in brackets.

Bond	Length	Bond	Length
C1–C2	1·36(3)	C21–C22	1·39(3)
C1–C6	1·38(3)	C22–C23	1·36(3)
C1–C34	1·54(3)	C23–C24	1·37(3)
C2–C3	1·40(3)	C23–C26	1·40(2)
C3–C4	1·37(3)	C24–C25	1·39(3)
C4–C5	1·36(3)	O26–C27	1·44(3)
C4–O7	1·42(2)	C27–C28	1·54(3)
C5–C6	1·38(3)	C28–C29	1·52(3)
O7–C8	1·36(2)	C29–C30	1·52(3)
C8–O9	1·17(3)	C30–C31	1·51(3)
C8–C10	1·52(3)	C31–C32	1·53(3)
C10–C11	1·39(3)	C32–C33	1·53(4)
C10–C15	1·38(3)	C34–C35	1·31(3)
C11–C12	1·39(3)	C34–O36	1·19(3)
C12–C13	1·36(3)	O35–C37	1·49(3)
C13–C14	1·36(3)	C37–C38	1·44(5)
C13–C16	1·51(3)	C37–C34	1·53(5)
C14–C15	1·39(3)	C38–C39	1·45(6)
C16–C17	1·53(3)	C39–C40	1·30(7)
C17–C20	1·51(3)	C40–C41	1·56(8)
C20–C21	1·38(3)	C41–C42	1·50(8)
C20–C25	1·35(3)	C42–C43	1·53(8)

the central core. The heptyloxy chain is fully extended and in the prolongation of the central core; the length of this moiety (C33 to C*37) is equal to 28·37 (4) Å. The significant torsion angles which entirely define the molecular conformation are given in table 4.

The phenyl rings ϕ_1 (C1 to C6), ϕ_2 (C10 to C15), ϕ_3 (C20 to C25) and the benzoate group are perfectly planar. The dihedral angles (ϕ_2/ϕ_1, ϕ_3/ϕ_2) are, respectively, equal to 62(1)° and 5(1)°. A drawing of the molecule is presented in figure 6; it shows significantly large ellipsoids for the chiral alkyl chain increasing from the C*37 chiral carbon to the C43 terminal methyl group. The projection of the structure on the (xOz) plane is shown in figure 7.

The molecules are arranged in an antiparallel way through the two-fold screw axes at $z = 0{\cdot}5$. The dihedral angles between the core of the parent molecule (x, y, z) and its crystallographic homologue ($-x$, $1/2+y$, $1-z$) is: ϕ_3'/ϕ_2 and ϕ_2'/ϕ_3 equal to 64(2)°. The alkoxy chains interact with the polyaromatic core of neighbouring molecules within the sheet. As has been already stressed [18, 24–26] the ether and the ester groups of neighbouring molecules strongly interact through their dipole moments: d(O7…O26′) = 4·55(2) Å and d(O9…O26′) = 4·66(2) Å, O26′ corresponding to the ($-x$, $1/2+y$, $1-z$) homologue. The present disposition of ether and ester groups is related to the mode II, according to Hori and Ohashi [18]. This corresponds to the maximum lateral overlapping of the cores and heptyloxy chains.

The molecular arrangement is of a smectic C type with sheets parallel to the (xOy) plane and a tilt angle (angle between the core axis with the Oz axis) close to 35°. The thickness of the sheets is quite close to the c parameter. The central part of the sheets is constituted by the polyaromatic cores prolonged by the heptyloxy chains; these parts interact through dipolar and van der Waals forces on the one side. On the other side the orthogonal chiral hexyl chains of neighbouring molecules, related through the 2_1 axis at $z = 0$ or 1, face each other and mutually interact through numerous van der Waals

Table 4. Significant torsion angles.

Atoms	Angle	Atoms	Angle
C2 –C1 –C34–O36	*trans*	C23–O26–C27–C28	*trans*
C3 –C4 –O7 –C8	121(2)	C34–O35–C37–C38	*trans*
C4 –O7 –C8 –C10	*trans*	O35–C37–C38–C39	−69(2)
C7 –C8 –C10–C11	*trans*	C44–C37–C38–C39	*trans*
C12–C13–C16–C17	97(2)	C37–C38–C39–C40	−153(5)
C13–C16–C17–C20	*trans*	C38–C39–C40–C41	*trans*
C16–C17–C20–C21	84(2)	C39–C40–C41–C42	160(5)

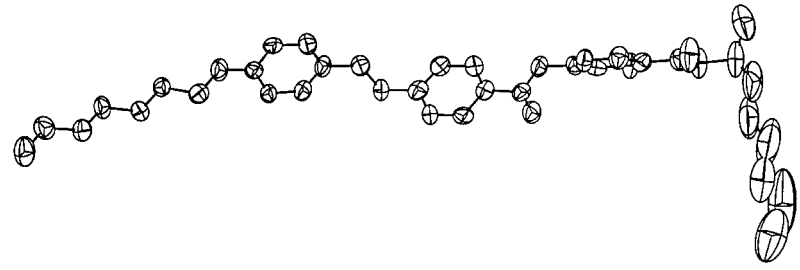

Figure 6. Snoopi drawing of the molecule; thermal ellipsoids are represented at the 50% probability level.

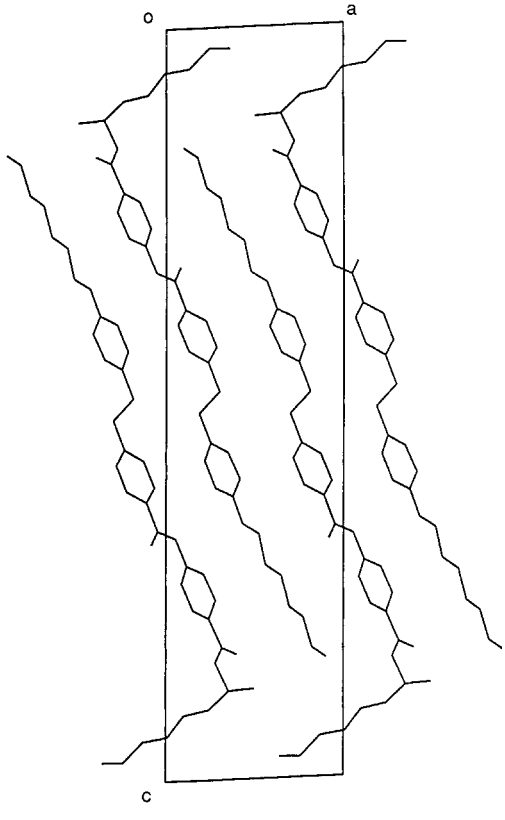

Figure 7. Projection of the structure on the (xOz) plane.

intersheet interactions. This special arrangement has been found in other chiral mesogenic compounds giving antiferroelectric mesophases. In particular, this is the case for the well known material MHPOBC [20] and the C7-Tolane [26] [(*S*)-4-(1-methylheptyloxycarbonyl)-phenyl 4-heptyloxytolane-4′-carboxylate].

The intersheet energy was found to be about $-35{\cdot}3$ kcal for the compound studied and only $-7{\cdot}1$ kcal for the C8F Tolane [33], with a large predominance of the van der Waals energy in both compounds. These values are in agreement with the molecular arrangement in the crystal. While the present molecules interact through their whole chiral groups, the molecules of the C8F Tolane interact only through their terminal methyl groups. For steric reasons it appears that there is an optimum length for the chiral chain: this should be about twice the mean width of the core which is about 10·2 Å; the length of chiral chain is close to $d[(C37\ldots C43)+r(CH_3)]=9{\cdot}2$ Å. In both MHPOBC and C7-Tolane molecules the chiral chain is also a 2-octyl chain [20, 26]. This could explain why the compounds with the chiral $CH(CH_3)C_2H_5$ group are unable to give a SmC_A^* mesophase.

8. Experimental

The compounds of the series II were prepared according to the scheme. The following examples are typical of the methods used. Infrared spectra were recorded on a Perkin Elmer 783 spectrophotometer and NMR spectra on a Bruker HV200 MHz spectrometer.

8.1. *4-Tetrahydropyranyloxy-4′-ethoxycarbonyltolane* ***3***

A mixture of 4-tetrahydropyranyloxyphenylacetylene **1** (8 g, 0·04 mol), ethyl 4-iodobenzoate **2** (11·6 g, 0·042 mol), TPP (0·3 g, 1·3 mmol) and diisopropylamine (120 ml), under nitrogen, was stirred and heated in an oil bath at 30°C until complete dissolution. Then the catalysts $PdCl_2$ (100 mg, 0·54 mmol) and $Cu(AcO)_2.H_2O$ (110 mg, 0·54 mmol) were added to this solution which was gradually heated to 80°C and maintained at this temperature for 3 h. After cooling to room temperature the salts were removed by filtration and washed well with ethyl acetate. The organic phase was dried over anhydrous sodium sulphate, filtered and evaporated. The residue was chromatographed on silica gel with toluene as eluent. The pure compound **3** was recrystallized from absolute ethanol. Yield 11·6 g (83·3%). δH (200 MHz, solvent $CdCl_3$, standard TMS): 0·90 (3H, t), 1·2–1·8 (4H, m), 3·5 (1H, m, THP), 3·9 (1H, m, THP), 5·0 (2H, q, CH_2OCO), 5·4 (2H, t, THP), 7–8 (8H, 4d, H arom). ν_{max} cm^{-1} (nujol) 2592, 2850, 1730, 1615, 1287, 1215, 850.

8.2. *4-Ethloxycarbonyl-4′-hydroxytolane* ***4***

The intermediate **3** (10 g, 0·029 mol) was dissolved in a mixture of CH_2Cl_2 (90 ml) and CH_3OH (150 ml). To this solution was added 4-toluenesulphonic acid (PTSA) (0·37 g) and the mixture was stirred at room temperature for 1 h. The solvent was evaporated and the pure phenol obtained by chromatography on silica gel, eluting with 8 : 2 heptane–ethyl acetate mixture. Yield 6·1 g (80%).

δH (200 MHz, solvent $CDCl_3$, standard TMS): 0·89 (3H, t), 3·1 (1H, s, OH), 5·0 (2H, q, CH_2OCO), 7–8 (8H, 4d, H arom). ν_{max} cm^{-1} (nujol) 3550, 2594, 2850, 1730, 1615, 1287, 1215, 850.

8.3. *1-(4-Ethyloxycarbonylphenyl)-2-(4-hydroxyphenyl)ethane* ***5***

To a solution of **4** (13·3 g, 0·05 mol) in ethyl acetate (300 ml) and ethanol 95% (50 ml) was added 0·4 g of Pd/C. Hydrogenolysis was carried out at room temperature. After filtration of the catalyst, the solvent was removed under reduced pressure and the desired phenol was recrystallized from a mixture of heptane and ethyl acetate (9:1). Yield 12·8 g (93%). δH (200 MHz, solvent $CDCl_3$, standard TMS): 0·85 (3H, t), 3·9 (4H, m, $2CH_2$), 4·8 (1H, s, OH), 5·0 (2H, q, CH_2OCO), 7–8 (8H, 4d, H arom). ν_{max} cm^{-1} (nujol) 3550, 2592, 2850, 1730, 1610, 1288, 1215, 850.

8.4. *1-(4-Nonyloxyphenyl)-2-(4-carboxyphenyl)ethane* ***6***

To a solution of potassium hydroxide (0·6 g, 0·012 mol) in 5 ml of water was added a solution of 100 ml of ethanol and **5** (2·7 g; 0·01 mol); 1-bromononane (2·3 g, 0·011 mol) in 50 ml of ethanol was then added dropwise. The solution was heated under reflux for 4 h. Then potassium hydroxide (3 g) in 3 ml of water was added to the cooled solution and the mixture was heated at reflux for a further 2 h. The solvent was removed and the mixture acidified with 10 ml of concentrated hydrochloric acid, 50 g of crushed ice and 50 ml of water. The solid was filtered off, washed well with water and recrystallized from absolute ethanol. Yield 2·6 g (66%). Six derivatives from heptyloxy to dodecyloxy of this series display the liquid crystal properties. They show SmC phases for the short chain members ($n = 7$–9), then SmC and SmI/F phases for the long chain homologues ($n = 10$–12) (table 5).

8.5. *(R)-4-(1-Methylheptyloxycarbonyl)phenyl 4-(4-nonyloxyphenyl)ethylbenzoate* ***II*** *($n = 9$)*

To a solution of (*R*)-1-methylheptyl 4-hydroxybenzoate (0·25 g, 1 mmol) in dichloromethane (5 ml) was added dicyclohexylcarbodiimide (DCC) (0·22 g, 1·1 mmol), 4-dimethylaminopyridine (DMAP) (10 mg) and acid **6** (0·40 g, 1·1 mmol). The mixture was stirred at room temperature overnight. It was then filtered and the solvent evaporated. The residue was chromatographed on silica gel with toluene as eluent. The desired compound was recrystallized from absolute ethanol. Yield 0·44 g (63%). δH (200 MHz, solvent $CDCl_3$, standard TMS): 0·86 (3H, t), 1·2–1·8 (27H, m) 2·9 (4H, m, $2CH_2$), 3·9 (2H, t, CH_2O), 5·1 (1H, m, CH*), 7–8·2 (12H, 6d, H arom). ν_{max} cm^{-1} (nujol), 2592, 2850, 1730, 1610, 1288, 1215, 850.

Table 5. Transition temperatures (°C) of intermediate acids, **6**.

	Phase						
n	Cr		SmI/F		SmC		I
7	•	135	—		•	195	•
8	•	127	—		•	194	•
9	•	124	—		•	192	•
10	•	120	•	160	•	191	•
11	•	118	•	160	•	190	•
12	•	114	•	160	•	189	•

References

[1] Meyer, R. B., Liebert, L., Strzeleski, L., and Keller, P., 1975, *J. Phys. Lett.*, **36,** L68.

[2] Clark, N. A., and Lagerwall, S. T., 1980, *Appl. Phys. Lett.*, **36,** 899.

[3] Chandani, A. D. L., Ouchi, Y., Takezoe, H., Fukuda, A., Furukawa, K., and Kichi, A., 1989, *Jpn. J. appl. Phys.*, **28,** 1261.

[4] Goodby, J. W., Patel, J. S., and Chin, E., 1992, *J. mater. Chem.*, **2,** 197.

[5] Fukuda, A., Takanishi, Y., Isozaki, T., Ishikawa, K., and Takezoe, H., 1994, *J. mater. Chem.*, **4,** 997; Nguyen, H. T., Rouillon, J. C., Cluzeau, P., Sigaud, G., Destrade, C., and Isaert, N., 1994, *Liq. Cryst.*, **17,** 571.

[6] Cluzeau, P., Nguyen, H. T., Destrade, C., Isaert, N., Barois, P., and Babeau, A., 1995, *Mol. Cryst. liq. Cryst.*, **260,** 69.

[7] Faye, V., Rouillon, J. C., Destrade, C., and Nguyen, H. T., 1995, *Liq. Cryst.*, **19,** 47.

[8] Booth, C. J., Dunmur, D. A., Goodby, J. W., Kang, J. S., and Toyne, K. J., 1994, *J. mater. Chem.*, **4,** 747.

[9] Suzuki, Y., Nonaka, O., Koide, Y., Okabe, N., Hagiwara, T., Kawamura, I., Yamamoto, N., Yamada, Y., and Katazume, T., 1993, *Ferroelectrics*, **147,** 109.

[10] Moritake, H., Shigeno, N., Ozaki, M., and Yoshino, K., 1994, *J. mater. Chem.*, **4,** 997.

[11] Nguyen, H. T., Babeau, A., Leon, C., Marcerou, J. P., Destrade, C., Soldera, A., Guillon, D., and Skoulios, A., 1991, *Liq. Cryst.*, **9,** 253.

[12] Nguyen, H. T., Zann, A., and Dubois, J. C., 1979, *Mol. Cryst. liq. Cryst.*, **53,** 43.

[13] Hori, K., and Ohashi, Y., 1988, *Bull. chem. Soc. Jpn.*, **61,** 3559.

[14] Hori, K., Takamatsu, M., and Ohashi, Y., 1988, *Ferroelectrics*, **55,** 485.

[15] Hori, K., and Ohashi, Y., 1989, *Bull. chem. Soc. Jpn.*, **62,** 3216.

[16] Hori, K., Takamatsu, M., and Ohashi, Y., 1989, *Bull. chem. Soc. Jpn.*, **62,** 1751.

[17] Hori, K., and Ohashi, Y., 1991, *J. mater. Chem.*, **1,** 667.

[18] Hori, K., and Ohashi, Y., 1991, *Mol. Cryst. liq. Cryst.*, **203,** 171.

[19] Hori, K., and Ohashi, Y., 1991, *Liq. Crystals*, **3,** 383.

[20] Hori, K., and Endo, K., 1993, *Bull. Chem. Soc. Jpn.*, **66,** 46.

[21] Hori, K., Kawahara, S., and Ito, K., 1993, *Ferroelectrics*, **147,** 91.
[22] Ito, K., Endo, K., Nemoto, T., Uekusa, M., and Ohashi, Y., 1994, *Liq. Cryst*., **17,** 747.
[23] Hori, K., and Kawahara, S., 1996, *Liq. Cryst*., **20,** 747.
[24] Zareba, I., Allouchi, H., Cotrait, M., Nabor, M.-F., Nguyen, H. T., and Destrade, C., 1996, *Ferroelectrics*, **180,** 117.
[25] Zareba, I., Allouchi, H., Cotrait, M., Chasseau, B., Nabor, M.-F., Destrade, C., and Nguyen, H. T., 1996, *Liq. Cryst*., **21,** 565.
[26] Zareba, I., Allouchi, H., Cotrait, M., Destrade, C., and Nguyen, H. T., 1996, *Acta Cryst*., **C52,** 441.
[27] Nguyen, H. T., Babeau, A., Rouillon, J. C., Sigaud, G., Isaert, N., Bougrioua, F., 1996, *Ferroelectrics*, **179,** 33.
[28] North, A. C. T., Philipps, D. C., and Matthews, F. S., 1968, *Acta Cryst*., **A24,** 351.
[29] Sheldrick, G. M., 1986, *Shelxl 86. Program for the Solution of Crystal Structures*, University of Gottingen, Germany.
[30] Sheldrick, G. M., 1993, *Shelxl 93. Program for the Refinement of Crystal Structures*, University of Gottingen, Germany.
[31] *International Tables for X-Ray Crystallography*, 1974 (Birmingham: Kynoch Press), Vol. IV.
[32] Dauber-Osguthope, P., Roberts, V. A., Osguthope, D. J., Wolff, J., Genest, M., and Hagler, A. T., 1988, *Proteins: Structure, Function and Genetics*, Vol. 4, p. 31.
[33] Laguerre, M., Zareba, I., Allouchi, H., Nguyen, H. T., and Cotrait, M., 1998, *Mol. Cryst. liq. Cryst*. (in the press).